Enhanced tribological properties of wind turbine engine oil formulated with flower-shaped MoS2 nano-additives

Mohamed Zoubair Saidi, Chaouki El Moujahid, Andreea Pasc, Nadia Canilho, Clara Delgado-Sanchez, Alain Celzard, Vanessa Fierro, Richard Kouitat-Njiwa, Tarik Chafik

Enhanced tribological properties of wind turbine engine oil formulated with flower-shaped MoS_2 nano-additives

Mohamed Zoubair Saidi,[1*] Chaouki El Moujahid,[1] Andreea Pasc,[2*] Nadia Canilho,[2] Clara Delgado-Sanchez,[3] Alain Celzard,[3] Vanessa Fierro,[3] Richard Kouitat-Njiwa,[4] and Tarik Chafik[1]

[1] Laboratoire de Génie Chimique et Valorisation des Ressources, Faculté des Sciences et Techniques de Tanger, Université Abdelmalek Essâadi, BP 416, Tanger, Maroc.

[2] L2CM UMR CNRS 7053, Université de Lorraine, 54506, Vandoeuvre-lès-Nancy, France

[3] IJL UMR 7198 CNRS, Université de Lorraine, 88000 Epinal, France

[4] IJL UMR 7198 CNRS, Université de Lorraine, 54000 Nancy, France

Corresponding author: med.zoubairs@gmail.com, andreea.pasc@univ-lorraine.fr

Highlights

- Flower shaped MoS_2 of about 150 nm were prepared via a hydrothermal method in a mixture of ethylene glycol/water (1: 4 volume ratio).
- Excellent dispersibility and long-term stability were achieved in wind turbine engine oil by surface hydrophobization of MoS_2 nanoparticles with alkyl-silane derivatives.
- A high deterministic relationship was found between the stability enhancement and the tribological efficiency.
- Grafting MoS_2 with longer alkyl chain (octadecyl *vs* octyl) lead to better tribological performance and higher lubricity power.

Abstract

Wind energy has become one of the most viable green and sustainable energy sources. A major concern of this sector is the damage of mechanical components and energy losses caused by repeated friction and wear, which lead to reduced efficiency and increased

maintenance costs. The development of new lubricant additives with high anti-wear properties and friction reduction capabilities is of paramount importance to ensure long service life and high efficiency of mechanical devices. Herein, flower-shaped MoS_2 nano-additives of about 150 nm were prepared under mild conditions through a hydrothermal process. Octyl- and octadecyltrichlorosilane were used as surface hydrophobization agents to enhance the colloidal stability of MoS_2 nano-additives formulations in wind turbine engine oil. Increasing the length of the alkyl chain grafted onto the particles improved the colloidal stability up to at least one year and, more importantly, resulted in the lowest friction and best wear reduction capabilities, as shown by the pin-on-disk tribometer and laboratory wear tests.

Graphical abstract

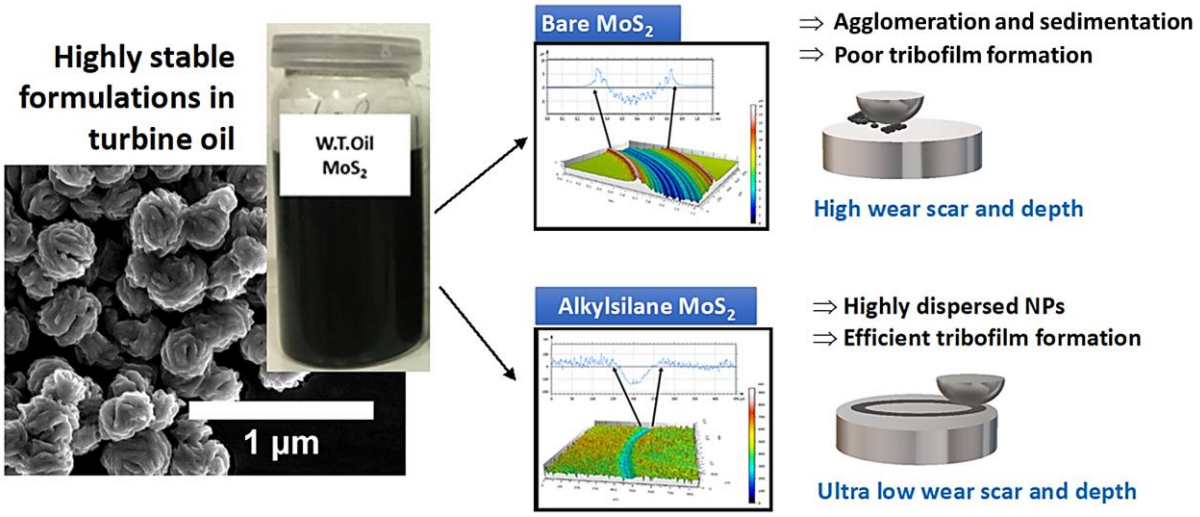

Keywords: MoS_2 nano-additives, Hydrothermal synthesis, Surface hydrophobization, Wind turbine lubricant, Formulation, Friction/Wear modifiers.

1. Introduction

Improving energy efficiency and sustainability in modern industry is one of the major global challenges facing the world today. Indeed, energy losses caused by excessive wear and friction in mechanical systems are estimated to account for more than 25% of the total energy

loss worldwide [1,2]. In the wind energy sector, maintenance costs account for about 30% of the total cost of the energy produced [3]. In particular, frequent critical failures and extensive maintenance work in wind turbines, mainly on gearboxes and bearing components, account for about 13% of total maintenance costs [4,5]. The origin of these failures is related to severe and unstable operating conditions such as high loads, extreme temperature, etc., which cause irreversible cumulative damage to mechanical components (micro-pitting, cracking, false brinelling and fretting corrosion, gear scuffing, …) and thus increase energy losses through heat generation [6]. Therefore, one of the most suitable and effective ways to overcome these failures and increase both economic and long-term benefits is the development of a new generation of lubricants that can ensure a long life and high efficiency of machine components and, consequently, a reduced maintenance time. The latest developments in lubrication technology have led to the design of new generations of lube oils based on advanced nanoparticles as lubricant additives (extreme pressure (EP), anti-wear (AW) and friction modifier (FM)). These advanced nano-additives are designed to react chemically with metal surfaces, forming protective film layers that reduce asperity contact as well as the coefficient of sliding friction. This prevents severe wear and seizure, overcoming the failure of vital engineering components and increasing the performance of mechanical systems under complex operating conditions, as well as increasing productivity by reducing energy consumption and increasing the reliability of contacting components [7-9].

Compared to conventional lubricant additives, nanoparticles exhibit many advantages [10], such as the multiple possibilities of film formation on many different types of surfaces, durability and low volatility to withstand high temperature conditions. Furthermore, nanomaterials have good tribological properties and excellent thermal conductivity. Their use as additives would lead to highly conductive nanofluids and thus limit overheating by homogenizing the temperature, which would be of high interest in extreme temperature

conditions. Thereby, thanks to the development of nanoscience and nanotechnologies, several studies have been carried out in order to examine the lubricating efficiency of different types of nanomaterials such as metals [11], metal oxides [12], metal dichalcogenides [13,14], borates [15] and so on, which has considerably widened the number of potential candidates to replace traditional additives. Among these advanced nanomaterials, molybdenum disulfide (MoS_2) is emerging as one of the most efficient anti-friction and extreme-pressure lubrication additives thanks to its special, graphite-like lubricating quality. The latter is based on its layered structure and low van der Waals force between layers allowing easy sliding, while its highly polarized sulfur atoms promote interaction between the particles and the metal surface, offering a great capacity to reduce friction and wear between opposing contact [16-18].

In addition, the tribological response of MoS_2 can be tuned by various intrinsic parameters such as morphology, size, crystal structure and concentration on their operating mechanism [19,20]. Tubular and spherical nanoparticles are considered the most suitable morphologies because of their high rolling and exfoliation capacities between sliding surfaces [21]. The size and concentration of nanoparticles in lubricating oils also have a great influence both on tribological performance and colloidal stability; large particles accelerate the sedimentation rate, while high concentration favors the collision and agglomeration of particles and, consequently, accelerate their sedimentation by gravitational effect [22,23]. Furthermore, nanoparticles are characterized by their high surface energy due to their high surface-to-volume ratio, which increases their ability to attract each other and agglomerate, and thus lose their lubricating properties.

In addition to size reduction, chemical modification of the surface of nanoparticles by dispersants or surfactants is considered an essential tool to improve colloidal stability by providing repulsive energy, which increases the distance between suspended nanoparticles and reduces their tendency to agglomerate. Furthermore, surface modification can generate a

lipophilic layer around the surface of the nanoparticles, which increases their compatibility with oils and therefore slows down their sedimentation rate and increases their colloidal stability.

Gulzar et al. [24] showed that the colloidal stability of lubricants containing CuO and MoS_2 nanoparticles modified with 1wt.% of oleic acid was achieved for more than 70h at room temperature. Yang et al. [25] indicated that the use of MoS_2 nanoparticles coated with PolyVinyl Pyrrolidone (PVP) produces a homogenous and stable system with negligible fluctuations for 48h in water, RPMI 1640 medium and PBS. Liu et al. [26] found that the use of CTAB-modified coral-like MoS_2 enhances the dispersion and stability of nanoparticles in liquid paraffin and also gives better results in improving lubrication performance due to its better oxidation resistance, better dispersion stability and easier exfoliation in liquid paraffin. Our group [27] investigated the effect of the morphology (1-5 μm platelets *vs* 600-800 nm spheres) of MoS_2 particles on their stability in poly-α-olefins oils (PAO) of different viscosities. The results revealed that the increase in oil viscosity and hydrophobization degree of the particles (related to the length of the hydrocarbon chain of the dispersant) produces extremely stable formulations in the long term. In addition, closer stability results were obtained for both the platelet-like particles and submicron spherical particles due to the drag forces applied by the lubricating medium on the surface of the particles, which were found to be greater for the platelet shape than for the spherical shape. Wu et al. [28] indicated that the dispersion stability of hydrothermally produced MoS_2 nanosheets in oil could be significantly enhanced with oleic diethanolamide borate (ODAB). Furthermore, the average friction coefficient, the average wear scar diameter and the performance at extreme pressure of ODAB-MoS_2-based oil were improved by approximately 27.9%, 22.9% and 17.4%, respectively, compared to the base oil. Kumari et al [29] successfully functionalized the surface of MoS_2 nanosheets with octadecylamine (ODA) and demonstrated that sulfur

vacancies and structural defects on the surface of MoS_2 nanosheets facilitate the grafting of ODA and ensure good dispersibility in mineral oil, resulting in a significant reduction in friction (48%) and wear (44%).

Our group also investigated [30] the colloidal stability and the tribological behavior of submicron solvothermal MoS_2 particles dispersed in poly-α-olefins (PAO) base oils as a function of the hydrophobization degree and viscosity of the oil and demonstrated that formulations containing 1wt.% of alkylsilane-modified MoS_2 nanoparticles remained highly stable (Turbiscan Stability Index < 1), even at high temperature (80°C). The tribological properties of the formulated poly-α-olefins lubricants also increased with the degree of hydrophobization of the MoS_2 particles.

Herein, we describe an efficient mixed hydrothermal method for the preparation of MoS_2 nanoparticles, with emphasis on the effect of the solvent to water ratio on the growth mechanism and the structural properties of the resulting particles. In order to examine their effect on friction and wear parameters in the presence of other common additives, the tribological potential of MoS_2 nanoparticles was evaluated in fully formulated commercial lubricating oil used for the lubrication of gearboxes in wind turbines. The results indicate excellent tribological performance and the presence of other additives did not alter the lubricating potential of these nanoparticles. Surface hydrophobization of these nanoparticles with alkylsilane groups provides high dispersibility and homogeneity in the oil system and further enhances the lubricity of the prepared formulations.

2. Experimental section

2.1. Syntheses of MoS_2 nanoparticles

MoS_2 nanoparticles were synthesized by a single-step hydrothermal approach using a Teflon-lined stainless steel autoclave filled with a mixture of water and ethylene glycol up to 60% of

its total volume (35 mL). In a typical procedure, 0.276 g of sodium molybdate ($Na_2MoO_4.2H_2O$), 0.106 g of sulfur powder (S) and 0.075 g of manganese dichloride were added to the autoclave filled with 21 mL of ethylene glycol - water mixture and maintained at 190°C for 24h. After natural cooling, the black product was separated from the solution by centrifugation, washed several times with distilled water and ethanol, and finally dried under vacuum at 60°C for 3h. Four volume ratios ($R_{EG\ /\ water}$) of ethylene glycol (EG) to water (W) in the mixture were used as follows: 1:1, 1:2, 1:3 and 1:4 and the syntheses were labelled EG1W1, EG1W2, EG1W3 and EG1W4 respectively.

2.2. Formulation of MoS_2-based nano-lubricants

In this study, fully formulated commercial oils used for the lubrication of wind turbine engines, are used as a continuous phase for the dispersion of 0.1 wt.% of MoS_2 nano-additives. 1 wt.% of alkyl trichlorosilane derivatives [octadecyltrichlorosilane (ODTS, $C_{18}H_{37}SiCl_3$) and octyltrichlorosilane (OTS, $C_8H_{17}SiCl_3$)] were added to enhance the colloidal stability of the prepared formulations. The formulations, with and without alkylsilane dispersants, were sonicated for 15 min using a 200W Sonopuls HD 2200 device used at 45% of its nominal power, then magnetically stirred for 2h at room temperature.

2.3. Characterization methods

X-ray diffraction (XRD) was performed using a Bruker D8 ADVANCE ECO diffractometer with Cu/Ka radiation (λ = 0.154 nm) and using a scanning rate of 0.04° s^{-1}. The morphology and structure of the MoS_2 samples were observed by scanning electron microscopy (SEM, Hirox SH-4000M) and transmission electron microscopy (TEM, JEOL 2100F). FTIR analysis was performed on a Jasco 410 spectrometer at a spectral resolution of 4 cm^{-1}. XPS analyses were recorded using a KRATOS Axis Ultra X-ray photoelectron spectrometer (Kratos Analytical, Manchester, UK) equipped with a monochromatic Al Kα X-ray source (hν =

1486.6 eV) operated at 150 W. The size distribution of the particles was measured by DLS on a Malvern Zetasizer 300HSA operating at an angle of 90°. The stability of the suspensions was determined using an optical analyzer (TURBISCAN LAB from Formulaction, L'Union, France), based on a light-scattering detection method. Tribological tests were performed using a CSM tribometer, with a pin-on-disk configuration. The ball used is in chrome steel type 100C6 with a diameter of 6 mm and the disk used is made of 304L stainless steel with a diameter of 30 mm and a height of 5 mm. The disks were "mirror polished" using finer silicon carbide abrasive disks in grades 400, 800 and 1200, in order to achieve the same finish and surface roughness for all samples. The topography of surfaces after the friction tests was studied using a smart WLI-extended optical 3D surface measurement system.

3. Results and discussion

3.1. Nanoparticles synthesis and characterization

The synthesis of the MoS_2 nanoparticles was carried out using a one-step hydrothermal method with a variable ethylene glycol to water volume ratio. All the products obtained were characterized by XRD, SEM and FTIR analysis, in order to determine the effect of ethylene glycol to water volume ratio on the intrinsic property of the products obtained.

The crystal structure and phase purity of the obtained samples were investigated by XRD. Fig. 1 displays the XRD patterns of the as-synthesized products as well as that of hexagonal 2H-MoS_2 (JCPD 37-1492). The XRD patterns of prepared samples (Fig. 1 (A-D)) are very similar and reveal the presence of broad diffraction peaks, characteristic of amorphous and disordered structure of MoS_2 materials. All diffraction patterns show two broad peaks towards 32° -33° and 57° - 58°, corresponding to the reflections of the (100) and (110) diffraction planes and indicating that the four prepared samples have the same atomic arrangement as that of 2H-MoS_2 along the basal planes [31]. However, the absence of the (002) plane in the XRD pattern of sample EG1W1 indicates that the stacked layered structure of MoS_2 did not occur

using an EG-water volume ratio of 1:1. Nonetheless, the appearance of a new broad peak centered at about 10° can be observed from the 1:2 volume ratio (sample EG1W2), and becomes more intense when the volume of ethylene glycol is reduced relative to water (Fig. 1. (B-D)). This peak could be assigned to the (002) plane of 2H-MoS_2 shifted to lower angles [32] and could corresponds to a periodic sequence of MoS_2 stacking layers along the c-axis. The shift of the (002) plane towards lower Bragg angles has been attributed to the interplanar expansion caused by molecular defects or strains due to layer curvature, as reported by other researchers [33-35].

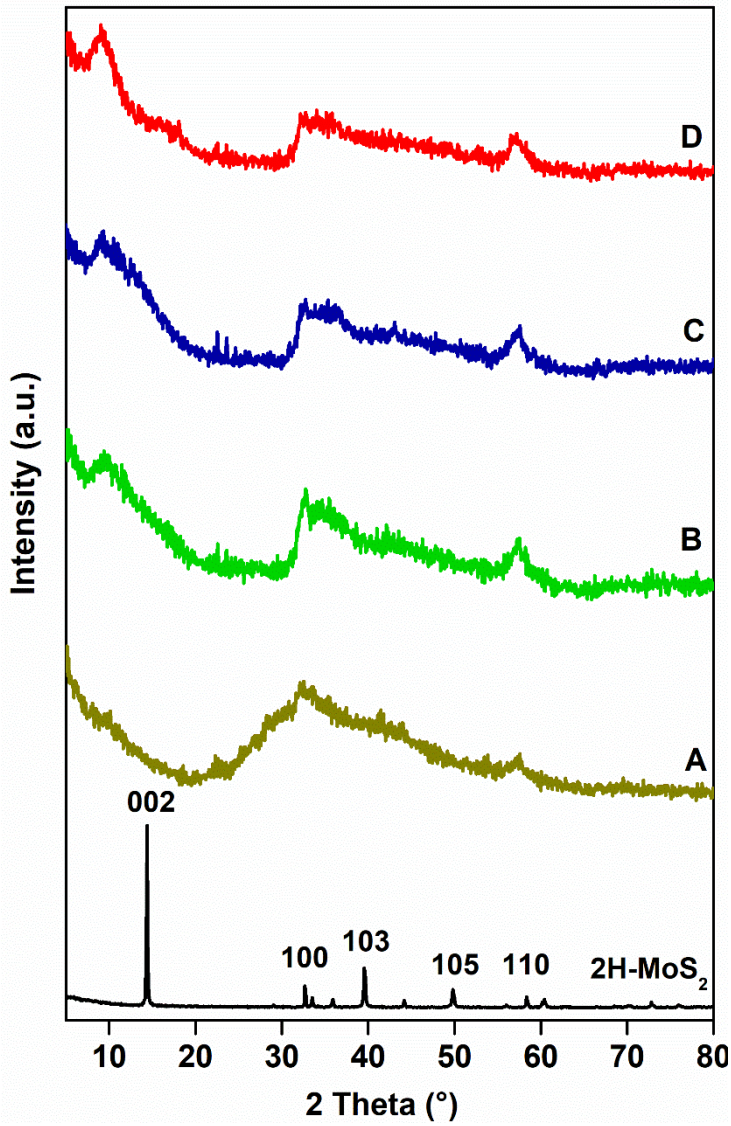

Fig. 1. XRD pattern of MoS_2 particles obtained from different ethylene glycol to water volume ratios. A) 1:1 (sample EG1W1), B) 1:2 (sample EG1W2), C) 1:3 (sample EG1W3), D) 1:4 (sample EG1W4) *vs* 2H-MoS_2.

The SEM images of the as-prepared products are shown in Fig. 2. The variation in the volume ratio of ethylene glycol to water, $R_{EG\ /\ water}$, initially shows a great influence on the size of the product obtained. Spherical nanoparticles with a relatively narrow size distribution and an average size of about 100-150 nm were obtained exclusively with an $R_{EG\ /H2O}$ of 1:4 (Fig. 2 (D)). By increasing the volume ratio of ethylene glycol, the size of the product obtained increases to more than 1 µm for particles resulting from an $R_{EG\ /\ water}$ of 1:1(Fig. 2 (A)). In addition to the impact on particle size, $R_{EG\ /\ water}$ has a strong effect on the morphology of the MoS_2 particles and on their agglomeration rate. For example, almost spherical particles with a diameter of 300 nm were obtained with the $R_{EG\ /\ water}$ of 1:3 (Fig. 2 (C)), while a $R_{EG\ /\ water}$ of 1:2 lead to highly agglomerated particles of irregular shape and inhomogeneous size (Fig. 2 (B)). However, a $R_{EG\ /\ water}$ of 1:1 produced irregular, agglomerated spheres with diameters greater than 1 µm, together with tubular and amorphous clusters (Fig. 2 (A)).

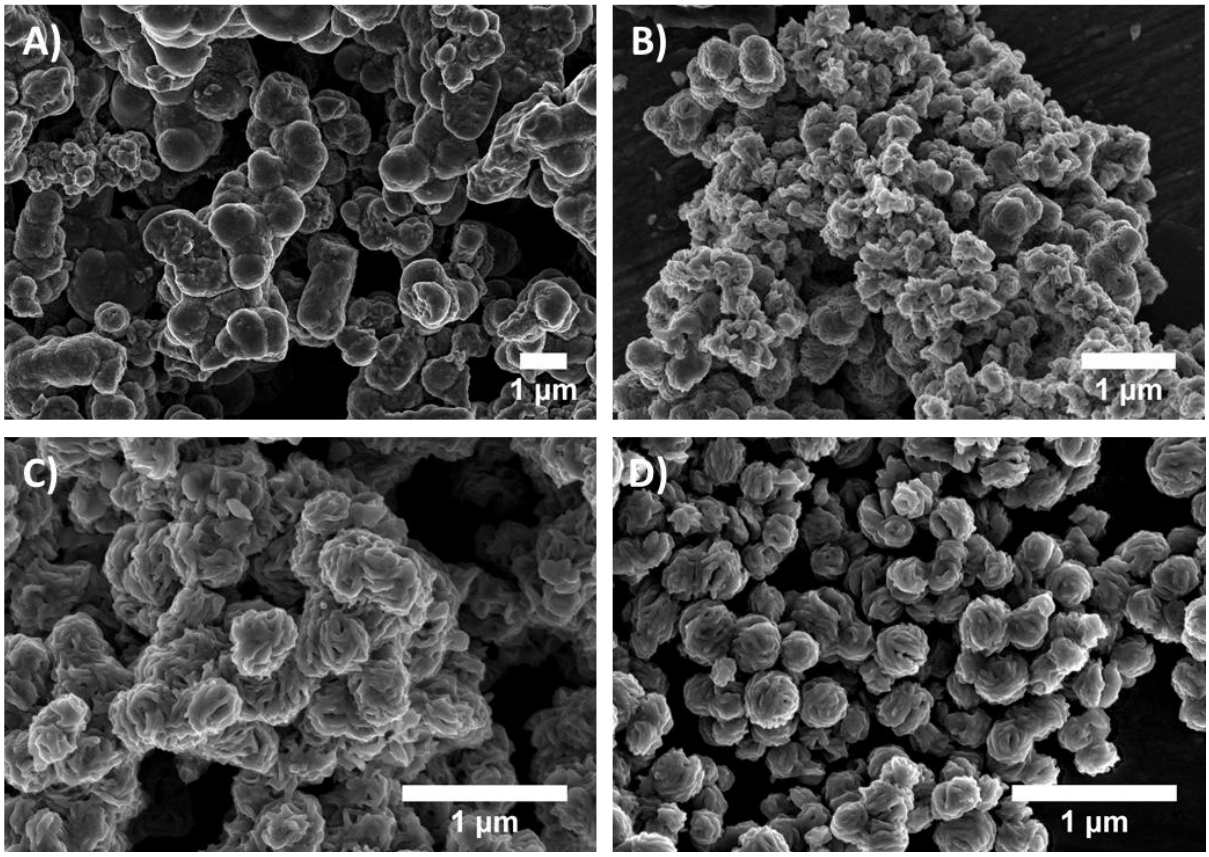

Fig. 2. SEM images of the as-synthesized materials obtained from different ethylene glycol to water volume ratios. A) 1:1 (sample EG1W1), B) 1:2 (sample EG1W2), C) 1:3 (sample EG1W3), D) 1:4 (sample EG1W4).

TEM images (Fig. 3) reveal the stacked lamellar structure of MoS_2 nanoparticles (sample EG1W4) and confirm their flower-shaped morphology with an interlayer spacing of 0.64 nm, which is in good agreement with the theoretical interplanar distance of the (002) plane for hexagonal MoS_2 (0.614 nm).

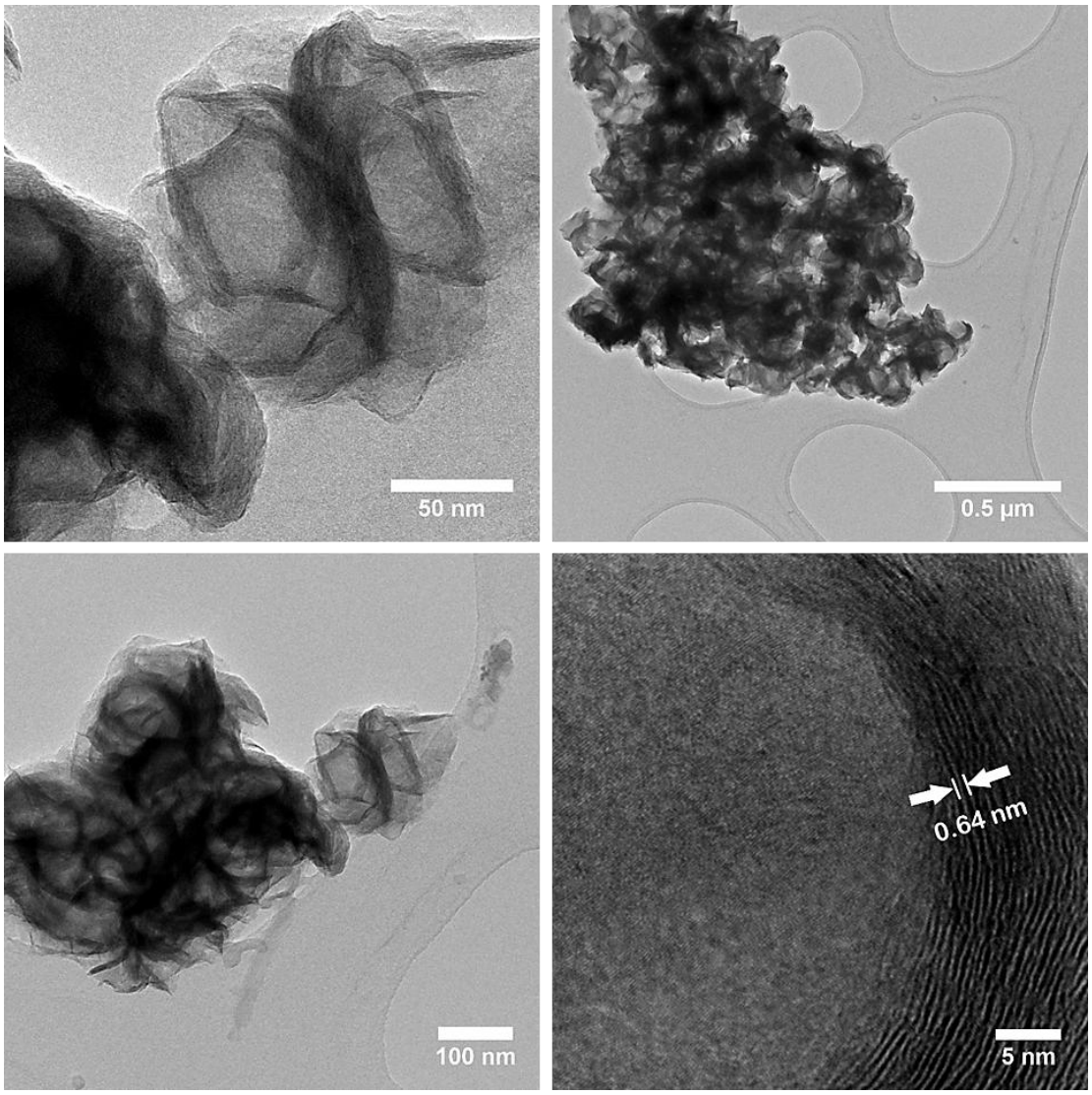

Fig. 3. TEM images of the MoS_2 nanoparticles (sample EG1W4).

To fully understand the mechanism of MoS_2 formation under these synthesis conditions, the effect of each reagent must be determined. It has been reported that EG, in addition to its use as a solvent, can also act as a (weak) reducing and stabilizing agent at the same time [36], while elemental sulfur and sodium molybdate are used as precursors of sulfur and molybdenum, respectively. The mechanism of MoS_2 formation begins with the reaction of elemental sulfur with EG to form H_2S by the following reactions [37]:

$$2\ HOCH_2\text{-}CH_2OH \rightleftarrows 2\ CH_3CHO + 2\ H_2O \qquad (1)$$

$$2\ CH_3CHO + S \rightleftarrows CH_3CO\text{-}COCH_3 + H_2S \qquad (2)$$

The H_2S formed in the reaction medium causes the gradual reduction of Na_2MoO_4 into Mo^{4+} ions, which, in the presence of subcritical water, are transformed into MoS_3 nuclei that are then decomposed into MoS_2, thermodynamically more stable [38]. Then, agglomeration and coalescence phenomena start spontaneously, until the MoS_2 nanoparticles reach their maximum size at which the particles are sufficiently stable [39]. Thus, the increase in the $R_{EG\ /H2O}$, could result in an increase of MoS_2 nuclei and thus to a higher nucleation rate and a continuous growth of the particles. On the contrary, a decrease in $R_{EG\ /H2O}$ could lead to reduced attraction forces between the nuclei during the growth process, thus creating an electrostatic barrier on the surface of the particles [39,40]. This barrier is added to that created by the ions Mn^{2+} and Cl^- coming from $MnCl_2$, which considerably increases the repulsion forces during the agglomeration and coalescence process and minimizes the dipole-dipole attractions between the particles [41]. These two electrostatic barriers lead to the formation of particles of smaller size.

All materials were characterized by FTIR and show similar spectra. As an example, Fig. 4 (A) shows the spectrum of EG1W4 nanoparticles. The first low intensity band observed around 465 cm^{-1} is assigned to the Mo-S bond [42], while those appearing at 664 cm^{-1} and 1048 cm^{-1} correspond to S_2^{2-} and sulfate species [43], respectively. A broad band at 801 cm^{-1} is also observed and may be due to the symmetrical and asymmetrical stretching vibrations of the cis dioxo MoO_2^{2+} group [44]. Other bands observed around 1624 cm^{-1}, 3220 cm^{-1} and 3425 cm^{-1} can be assigned to the water adsorbed on the surface of these nanoparticles [45].

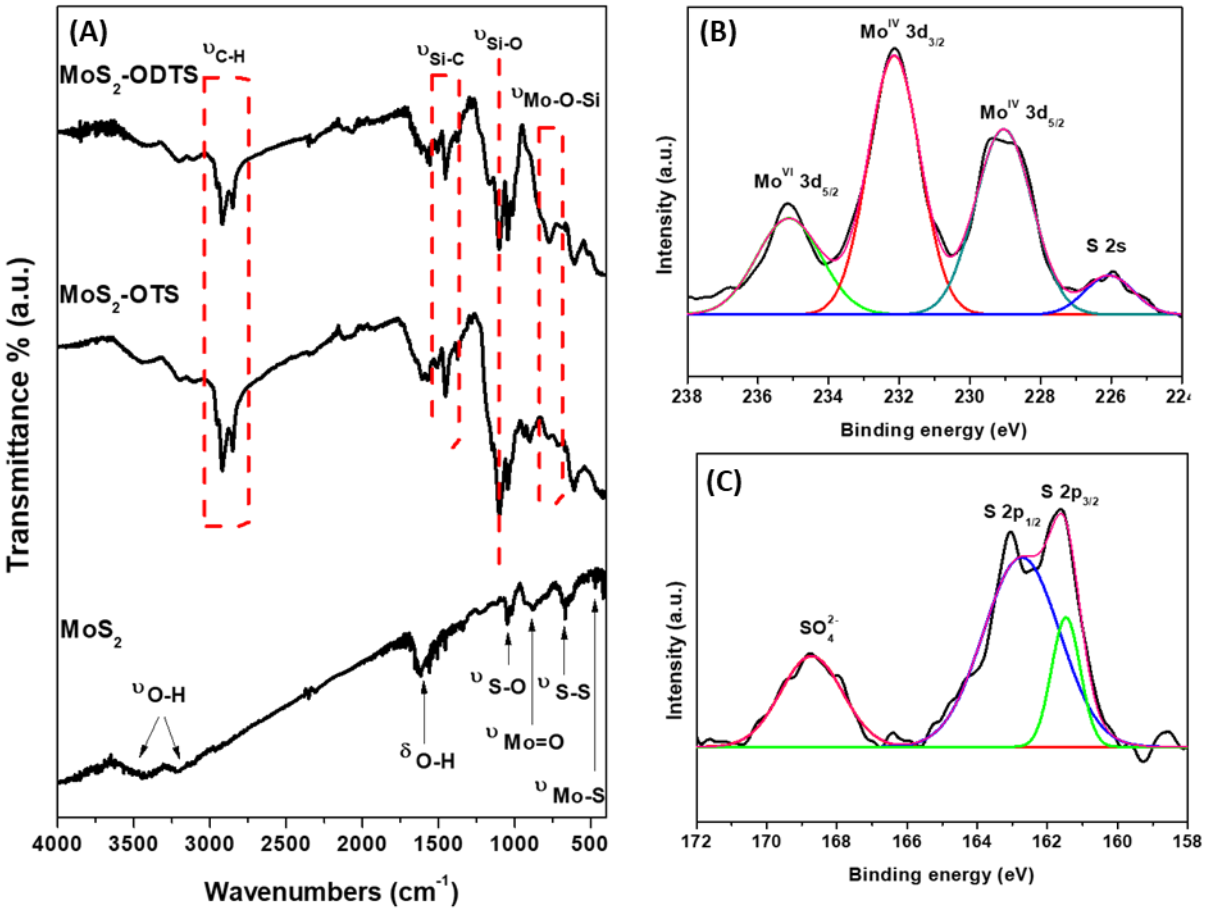

Fig. 4. (A) FTIR spectra of MoS_2 nanoparticles with and without alkyl-silane derivatives, and XPS spectra of Mo 3d (B), and S 2p (C).

Further insights in the chemical composition and atomic valence states of the as-synthesized MoS_2 nanoparticles were obtained from XPS analysis. Fig. 4(B) displays the Mo 3d spectrum with four peaks, two of which are predominant at 232.14 eV and 229.02 eV that can be assigned to Mo 3d3/2 and Mo 3d5/2 doublets of Mo^{4+}, respectively [46]. The peak at 235.14 eV can be attributed to Mo 3d5/2 of Mo^{6+}, which implies the presence of an oxide state resulting from the oxidation of MoS_2 nanoparticles in air [47]. Finally, a weak peak at 226.13 eV is ascribed to S 2s. As for the S 2p spectrum (Fig. 4(C)), the two mains doublets appeared at binding energies of 161.63eV and 163.04 eV and are due to S 2p3/2 and S2 p½ doublet of S^{2-}. The peak at 168.78eV indicates the existence of SO_4^{2-} species and confirms the partial

oxidation of MoS_2 surface in contact with air [48]. The binding energies of Mo 3d and S 2p are in good agreement with the reported values for MoS_2 particles [49,50,29].

3.2. Surface modification and nano-lubricant preparation

The surface modification of the MoS_2 nanoparticles was conducted in the commercial gearbox oil of a wind turbine. 0.1 wt.% of the prepared MoS_2 nanoparticles with and without alkyltrichlorosilane were added to the oil. The surface modification of MoS_2 nanoparticles was first investigated by FTIR analysis. The infrared spectra of alkylsilane-modified MoS_2 nanoparticles (Fig. 4 (A)) indicate the appearance of two new bands located at 2847 and 3923 cm^{-1} for both functionalized materials, attributed to the stretching vibration of methylene groups from the alkylsilane dispersants [27]. In addition, the band observed at 1452 cm^{-1} could be assigned to the Si-C vibration, whereas those appearing at about 1001 and 761 cm^{-1} were attributed to Si-O and Mo-O-Si vibrations, respectively [30]. Compared to the infrared spectra of unmodified MoS_2 nanoparticles, the presence of these news bands confirmed the chemisorption of alkyltrichlorosilane molecules on the surface of MoS_2 nanoparticles.

The prepared formulations, with modified and unmodified nanoparticles, were left at rest and visually inspected daily for 20 days, and then monthly, in order to follow their colloidal stability as a function of time (Fig. 5). Visual monitoring of the sedimentation process indicated that all formulations remained stable, and no changes were visually observed even after 1 year after their preparation. In order to demonstrate the effect of the dispersants used on the colloidal stability and agglomeration tendency of the MoS_2 nanoparticles dispersed in commercial oil used in wind turbines, the hydrodynamic size and the particle size distribution were investigated by dynamic light scattering (Fig. 6). However, the high viscosity of commercial oil prevents the movement of the particles, and therefore the measurement of their hydrodynamic size by the DLS technique. Thus, a 10-fold dilution was made in a less

viscous base oil (PAO4). The results obtained are shown in Fig. 6 and indicate the power of alkylsilane moieties in reducing the agglomeration rate of blended oil/nano-MoS_2 systems. The addition of 1 wt.% of dispersants resulted in a finer, monodisperse particle size distribution. Furthermore, the MoS_2-ODTS formulation presents the smallest average size and the most homogenous particle distribution compared to bare MoS_2 and MoS_2-OTS formulations, confirming the effect of the length of the hydrocarbon chain (hydrophobization rate) in improving colloidal stability.

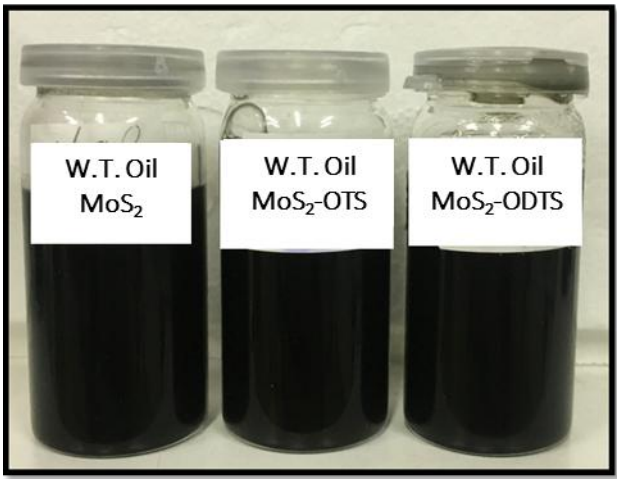

Fig. 5. Images of blended wind turbine oil and MoS_2 nanoparticles with and without alkyl-silane dispersants after 20 days of preparation.

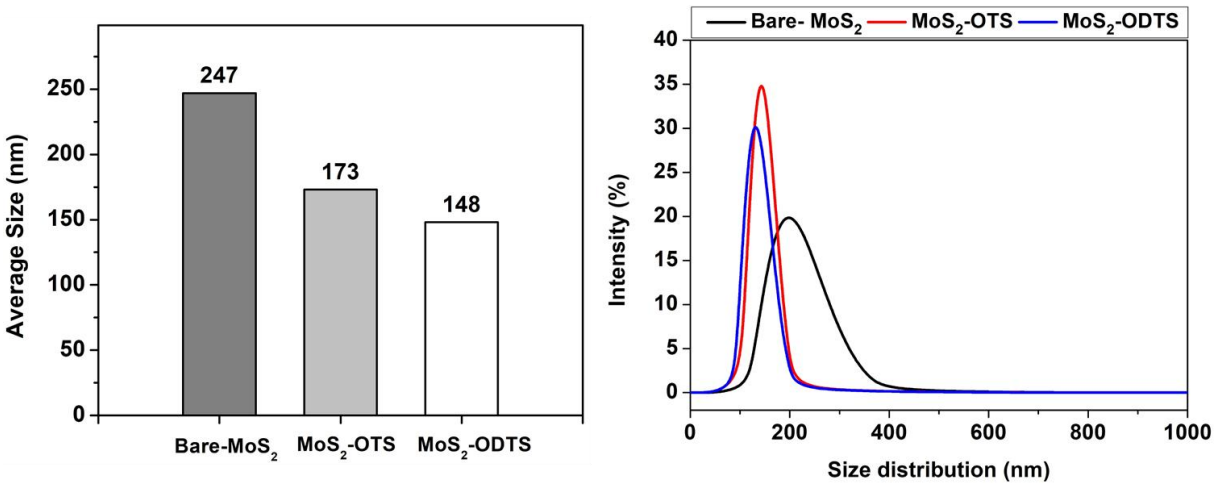

Fig. 6. Average particle size and particle size distribution of modified and unmodified MoS_2 nanoparticles.

In order to further evaluate the effect of surface modification of MoS_2 nano-additives on their colloidal stability, the prepared formulations were studied by Turbiscan analysis. Based on the variation rate in transmission and backscattering intensity from the initial point, the Turbiscan stability index (TSI) could be monitored. A high stability index reflects large variations between transmission and/or backscattering intensity, indicating poor stability of the dispersions system.

The TSI variations of the mixture containing modified and unmodified MoS_2 nanoparticles at room temperature (25 °C) are given in Fig. 7. All formulations contain the same amount of additive. In general, the TSI of the mixture containing bare nanoparticles shows a slight increase from the beginning of the test to reach about 5 after 8 days of testing. The addition of 1 wt.% of ODTS / OTS remarkably improves the stability of these particles and leads to extremely stable formulations with TSI values less than 0.5 at the end of the test. To summarize, in the same type of oil, nanoparticles modified with alkyltrichlorosilanes always exhibit better stability compared to bare particles, which confirms the positive effect of these dispersants, ensuring good dispersibility and significantly reducing the size of the resulting agglomerates. The strong improvement in the colloidal stability of the formulation containing the modified nanoparticles could be due to the steric effect of the dispersant hydrocarbon chains, reducing the forces of attraction between the particles and limiting their tendency to agglomerate by creating a steric barrier. This barrier becomes stronger as a function of the length of the hydrocarbon chain of the dispersant, as proved by DLS analysis and confirmed by the extreme stability obtained for the formulation based on MoS_2 modified with ODTS moieties.

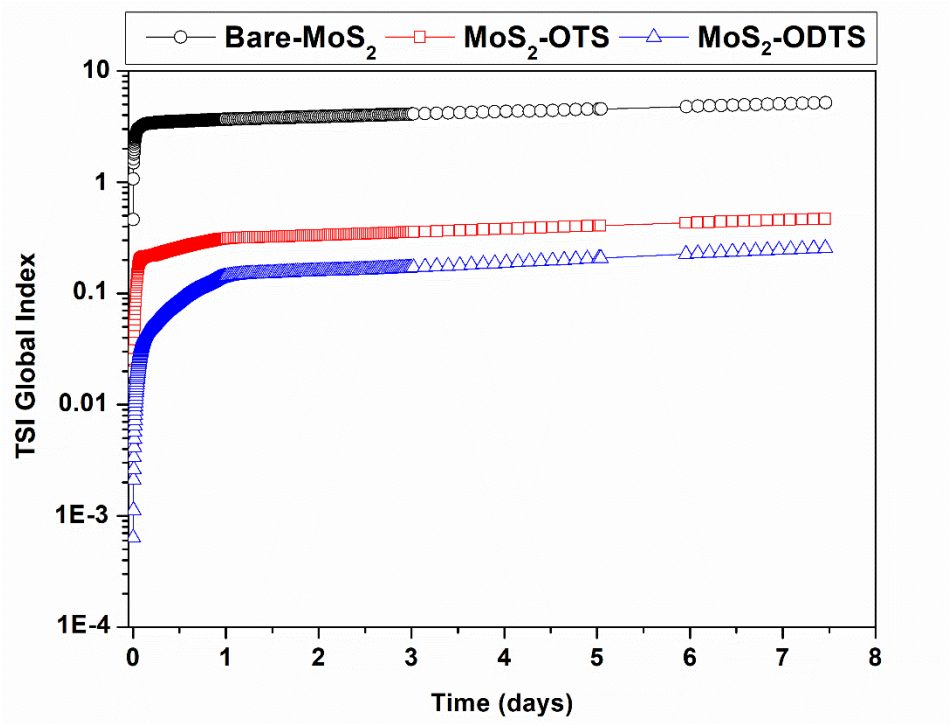

Fig. 7. Turbiscan stability index as function of time.

3.3. Tribological behavior of formulations based on MoS_2

The friction-reducing and anti-wear properties of MoS_2 nanoparticles dispersed in wind turbine engine oil, with and without dispersants, were evaluated using a pin-on-disk laboratory tribometer under different loads (1N and 10N, corresponding respectively to about 450 MPa and 980 MPa mean contact pressure).

3.3.1. Friction reduction abilities

Fig. 8 shows the anti-friction behavior of the different formulations at a load of 1N. The results obtained show that the commercial wind turbine oil has the highest friction coefficient with an average value of approximately 0.190. The addition of 0.1 wt.% of MoS_2 nanoparticles produced a reduction in the friction coefficient of 14.5% (0.162). Nevertheless, the lowest and most stable friction coefficients were obtained for formulations containing the nanoparticles functionalized with alkylsilane groups. Indeed, the addition of the particles

grafted with OTS (-C8) reduces the average friction coefficients up to 41.1%, while the formulations based on MoS_2-ODTS exhibit the lowest average friction coefficients, with a reduction of up to 47.5% compared to wind turbine oil. By increasing the load to 10N (Fig. 9), the wind turbine oil exhibits variations in the friction coefficient at the beginning of the test before stabilizing at about 0.14 after 200 cycles. The addition of the MoS_2 nanoparticles tends to decrease the friction coefficient at the beginning of the test. However, after 200 cycles, the friction coefficient increases to reach maximum values of up to 0.250. The average coefficient calculated at the end of the test is about 0.194, which shows an increase of about 35.6% compared to wind turbine oil. Again, the lowest and most stable friction coefficients are obtained with the formulations containing the alkylsilane-modified nanoparticles. The average friction coefficient obtained with ODTS and OTS at 10N are almost identical, around 0.1, exhibiting a reduction of about 30% compared to wind turbine oil.

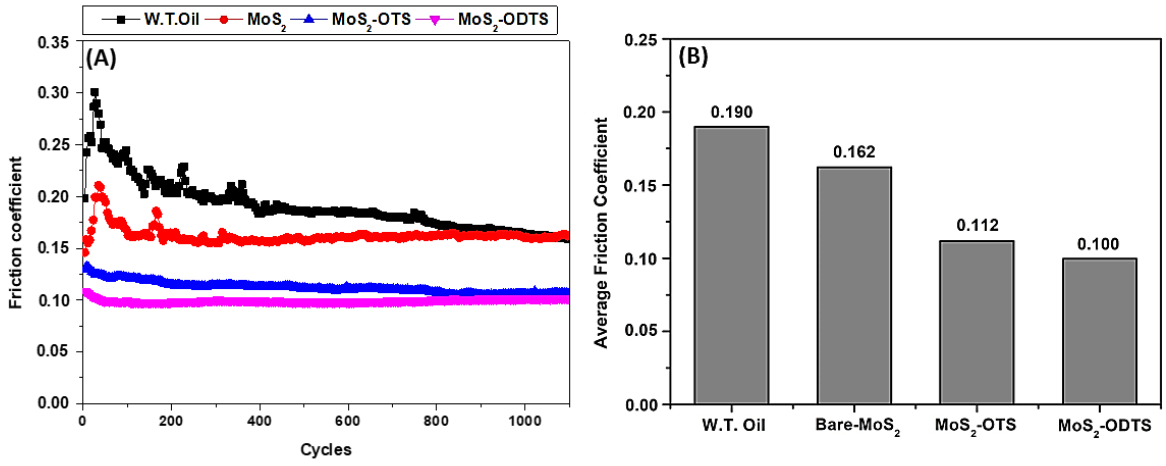

Fig. 8. Friction-reducing behavior (A) and average Friction coefficient (B) of wind turbine oil under a load of 1N.

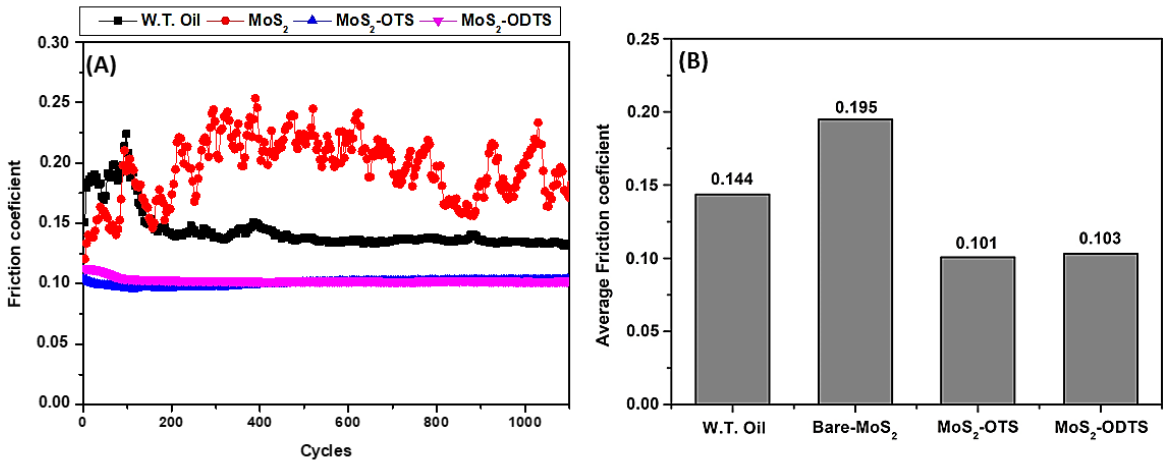

Fig. 9. Same as Fig. 8, but under 10N.

It has already been reported that for certain types of anti-wear and friction-reducing additives, thermal activation is required to trigger their lubricating power [32,33]. This may explain the instability of the friction behavior observed at the beginning of the test for wind turbine oil, and its stability after the 200 cycles. Conversely, the use of MoS_2 nanoparticles does not require any time for the formation of the tribofilm, but their strong aggregation tendency leads to the formation of large particles, which limits their passage to the contact surfaces. The reduction in the number of particles between the moving surfaces leads to the formation of a thin tribofilm that degrades rapidly. This can be confirmed by a simple comparison of the friction behavior observed at both 1N and 10N of bare MoS_2 nanoparticles with that of their analogs functionalized by alkylsilane groups. The functionalization of the surface of these nanoparticles leads to an improvement of their stability by reducing their agglomeration tendency, enabling them to exhibit again the best friction-reducing properties, with average values not exceeding 0.1 for the entire duration of the test.

3.3.2. Anti-wear properties

The effectiveness of a lubricant depends not only on its ability to reduce friction, but also on its ability to decrease wear rates and minimize surface damage between contacting

components. To further explore the effect of MoS_2 nano-additives on contact sliding and surface damage, the surface topography was evaluated using a 3D optical surface measurement system. The analysis of the wear track surface (Fig. 10) indicates, in the case of pristine engine oils, the presence of grooves, scars and debris on the contact track. The wear depth obtained at a load of 10N is approximately 6.57 µm (Fig. 11). However, the addition of 0.1 wt.% of bare MoS_2 nanoparticles shows a slight reduction in wear depth of about 4.3% compared to the original oil. While the addition of nanoparticles modified with OTS and ODTS leads to significant reductions of up to 95.44% and 97.87 %, respectively. In addition, the comparison of 3D images of the wear tracks obtained with the different formulations confirms the negative effect of nanoparticles agglomeration on their performance and tribological efficiency as lubricant additives. They also show that the improvement in dispersibility and stability of these nano-additives dispersed in lubricant oils is a key and determining factor of their tribological power, leading not only to the improvement of their friction-reducing properties but also to a significant decrease in both the depth and width of wear.

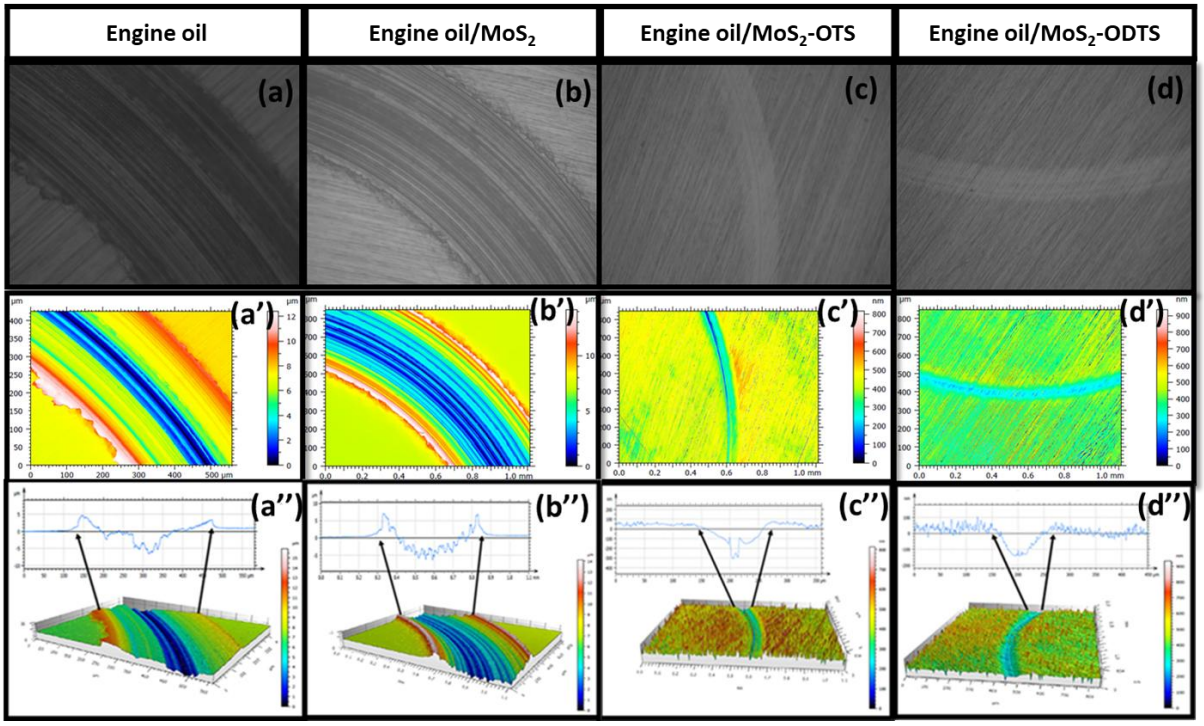

Fig. 10. Optical micrographs, pseudo-color view, 3D view and profile curve of wear track: (a, a', a'') Engine oil, (b, b', b'') Engine oil/MoS_2, (c, c', c'') Engine oil/ MoS_2-OTS, (d, d', d'') Engine oil/MoS_2-ODTS.

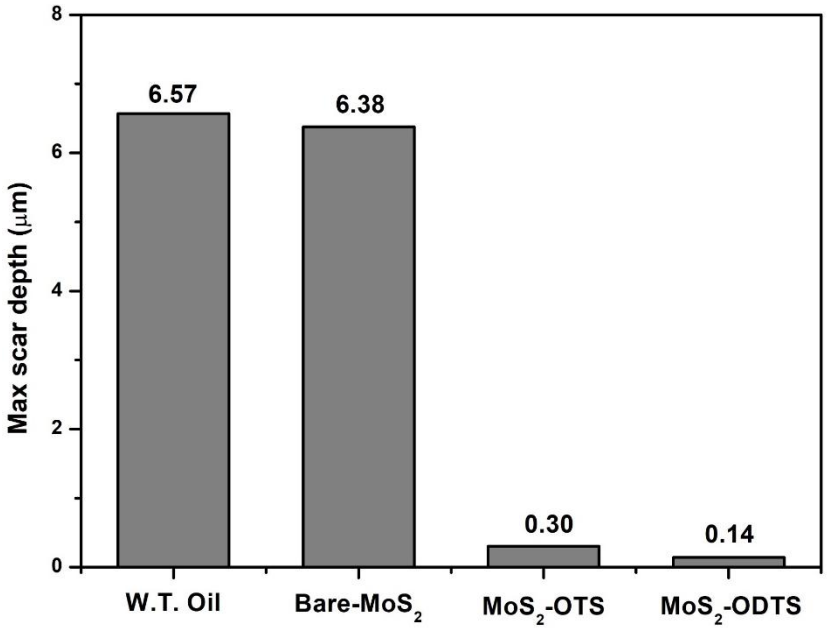

Fig. 11. Maximum scar depth obtained with different formulations in wind turbine oil.

Conclusion

In summary, the present study revealed that the variation in the ethylene glycol to water volume ratio subjected to hydrothermal treatment has a strong influence on the morphology and size of the MoS_2 nanoparticles obtained. Indeed, flower-shaped MoS_2 nanoparticles with an average size of about 150 nm have been obtained with a EG / W volume ratio of 1:4. By increasing the EG fraction, the particle size increases, and its morphology becomes less homogeneous and the rate of aggregation more important.

Alkyltrichlorosilane derivatives have proven their effectiveness as dispersing agents, leading to excellent dispersibility and long-term stability with TSI values below 0.5 in a fully formulated wind turbine oil. Subsequently, the evaluation of the tribological behavior of formulations with and without modified and unmodified MoS_2 nano-additives first shows that the excessive tendency of bare MoS_2 nanoparticles to agglomerate leads to the formation of

large particles, acting as abrasive bodies between the sliding surfaces, and thus leading to the deterioration of their lubricity. On the other hand, improving the dispersibility and the stability of these nano-additives in lubricating oils has proven to be a key and determining factor in improving their tribological efficiency, leading not only to an improvement in their friction-reducing properties, but also to a significant decrease in depth and width of wear. More importantly, MoS_2 nanoparticles modified with octadecyl moieties have been most effective in reducing the friction and wear coefficients when added to wind turbine engine oil under laboratory conditions. This resulted in a reduction of more than 30% in the friction coefficient and up to 97% in the maximum wear depth.

Acknowledgements

The authors thank the institute IRESEN/Morocco (Project Innowind13 Nanolubricant) for its financial support and for the scholarship awarded to M.Z. Saidi. The authors also thank S. Haloui (Innovation and Development Center, University of Abdelmalek Essaadi) for performing X-ray measurements and Ovidiu Ersen and Dris Ihiawakrim (IPCMS, University of Strasbourg) for performing TEM analysis.

References

[1] T. Luo, X. Chen, L. Wang, P. Wang, C. Li, H. Zeng, and B. Cao, Green laser irradiation-stimulated fullerene-like MoS_2 nanospheres for tribological applications. Tribol. Int., 122 (2018) 119-124, doi:10.1016/j.triboint.2018.02.040.

[2] K. Holmberg, A. Erdemir, Influence of tribology on global energy consumption, costs and emissions. Friction, 5 (2017) 263-284, doi:10.1007/s40544-017-0183-5.

[3] M. Shafiee, J.D. Sørensen, Maintenance optimization and inspection planning of wind energy assets: Models, methods and strategies. Reliab. Eng. Syst. Safe. 192 (2017), doi:10.1016/j.ress.2017.10.025.

[4] C. Peeters, P. Guillaume, J. Helsen, Vibration-based bearing fault detection for operations and maintenance cost reduction in wind energy. Renew. Energ., 116 (2018) 74–87. doi:10.1016/j.renene.2017.01.056.

[5] B. Graca, J. Castro, R. Martins, C. Fernandes, J. Seabra, Failure and oil analysis in wind turbine gearboxes, Proceedings of the International Conference BALTTRIB', 2013.

[6] C. Nutakor, D. Talbot, A. Kahraman, An experimental characterization of the friction coefficient of a wind turbine gearbox lubricant, Wind Energy, 22 (2019) 509-522, doi:10.1002/we.2303.

[7] J.C. Spear, B.W. Ewers, J.D. Batteas, 2D-Nanomaterials for controlling friction and wear at interfaces. Nano Today, 10 (2015) 301-314, doi: 10.1016/j.nantod.2015.04.003.

[8] A.K. Rasheed, M. Khalid, W. Rashmi, T.C.S.M. Gupta, A. Chan, Graphene based nanofluids and nanolubricants – Review of recent developments. Renew. Sust. Energ. Rev., 63 (2016) 346-362, doi:10.1016/j.rser.2016.04.072.

[9] L.C. Liu, M. Zhou, X. Li, L. Jin, G.S. Su, Y.T. Mo, L.C. Li, H.W. Zhu, Y. Tian, Research progress in application of 2D materials in liquid-phase lubrication system, Materials, 11 (2018), doi: 10.3390/ma11081314.

[10] H. Spikes, Friction modifier additives. Tribol. Lett., 60 (2015) 1–26, doi: 10.1007/s11249-015-0589-z.

[11] J. Padgurskas, R. Rukuiza, I. Prosyčevas, R. Kreivaitis, Tribological properties of lubricant additives of Fe, Cu and Co nanoparticles. Tribol. Int. 60 (2013) 224-232, doi:10.1016/j.triboint.2012.10.024.

[12] M.K.A. Ali, H. Xianjun, L. Mai, C. Qingping, R.F. Turkson, C. Bicheng, Improving the tribological characteristics of piston ring assembly in automotive engines using Al_2O_3 and TiO_2 nanomaterials as nano-lubricant additives, Tribol. Int., 103 (2016) 540-554, doi:10.1016/j.triboint.2016.08.011.

[13] Y. Liu, C. Li, J. Yang, Y. Yu, X. Li, Synthesis and Tribological Properties of Tubular NbS_2 and TaS_2 Nanostructures, Chinese J. Chem. Phys., 20 (2007) 768-772, doi:10.1088/1674-0068/20/06/768-772.

[14] B.J. Irving, P. Nicolini, T. Polcar, On the lubricity of transition metal dichalcogenides: an ab initio study. Nanoscale, 9 (2017) 5597-5607, doi:10.1039/c7nr00925a.

[15] H.R.M. Saffari, R. Soltani, M. Alaei, M. Soleymani, Tribological properties of water-based drilling fluids with borate nanoparticles as lubricant additives. J. Petrol. Sci. Eng. 171 (2018) 253 259, doi:10.1016/j.petrol.2018.07.049.

[16] X. Wu, K. Gong, G. Zhao, W. Lou, X. Wang, W. Liu, Surface modification of MoS_2 nanosheets as effective lubricant additives for reducing friction and wear in Poly-α-olefin. Ind. Eng. Chem. Res., 57 (2018) 8105–8114, doi: 10.1021/acs.iecr.8b00454.

[17] Z. Chen, Y. Liu, S. Gunsel, J. Luo, Mechanism of antiwear property under high pressure of synthetic oil-soluble ultrathin mos_2 sheets as lubricant additives. Langmuir, 34 (2018) 1635-1644. doi: 10.1021/acs.langmuir.7b03851

[18] M. Kalin, J. Kogovsek and M. Remskar, Mechanisms and improvements in the friction and wear behavior using MoS_2 nanotubes as potential oil additives, Wear, 280-281 (2012) 36-45, doi: 10.1016/j.wear.2012.01.011.

[19] E.Z. Hu, Y. Xu, K.H. Hu, X.G. Hu, Tribological properties of 3 types of MoS_2 additives in different base greases, Lubr. Sci., 29 (2017) 541–555, doi: 10.1002/ls.1387.

[20] P. Rabaso, F. Ville, F. Dassenoy, M. Diaby, P. Afanasiev, J. Cavoret, T. Le Mogne, Boundary lubrication: Influence of the size and structure of inorganic fullerene-like MoS_2 nanoparticles on friction and wear reduction, Wear, 320 (2014) 161-178, doi: 10.1016/j.wear.2014.09.001.

[21] A. Tomala, M.R. Ripoll, J. Kogovšek, M. Kalin, A. Bednarska, R. Michalczewski, M. Szczerek, Synergisms and antagonisms between MoS_2 nanotubes and representative oil additives under various contact conditions, Tribol. Int., 129 (2018), 137-150, doi: 10.1016/j.triboint.2018.08.005.

[22] P. Wu, W. Li, T. Ge, Y. Feng, Z. Liu, Z. Cheng, Preparation and tribological properties of chemically decorated MoS_2 nanosheets with oleic diethanolamide, Lubr. Sci., 31 (2018), 41-50, doi:10.1002/ls.1444.

[23] C.P. Koshy, P.K. Rajendrakumar, M.V. Thottackkad, Evaluation of the tribological and thermo-physical properties of coconut oil added with MoS_2 nanoparticles at elevated temperatures, Wear, 330-331 (2015) 288-308, doi:10.1016/j.wear.2014.12.044.

[24] M. Gulzar, H. Masjuki, M. Varman, M. Kalam, R. Mufti, N. Zulkifli, R. Yunus, R. Zahid, Improving the AW/EP ability of chemically modified palm oil by adding CuO and MoS_2 nanoparticles, Tribol. Int., 88 (2015) 271-279, doi:10.1016/j.triboint.2015.03.035.

[25] H. Yang, J. Zhao, C. Wu, C. Ye, D. Zou, S. Wang, Facile synthesis of stable colloidal MoS_2 nanoparticles for combined tumor therapy, Chem. Eng. J., 351 (2018) 548-558, doi: 10.1016/j.cej.2018.06.100.

[26] L. Liu, Z. Huang, P. Huang, Fabrication of coral-like MoS_2 and its application in improving the tribological performance of liquid paraffin. Tribol. Int., 104 (2016) 303–308, doi: 10.1016/j.triboint.2016.09.013.

[27] M.Z. Saidi, H. Akram, O. Achak, C. El Moujahid, A. El Mouakibi, N. Canilho, C. Delgado- Sánchez, A. Celzard, V. Fierro, A. Pasc, T. Chafik, Effect of morphology and hydrophobization of MoS_2 microparticles on the stability of poly-aolefins lubricants, Colloid. Surface A., 572 (2019) 174–181, doi: 10.1016/j.colsurfa.2019.04.003.

[28] P.-R. Wu, W. Li, Y.-M. Feng, T. Ge, Z. Liu, Z.-L. Cheng, Fabrication and tribological properties of oil- soluble MoS_2 nanosheets decorated by oleic diethanolamide borate, J. Alloy. Compd., 770 (2019) 441-450, doi: 10.1016/j.jallcom.2018.08.156.

[29] S. Kumari, A. Chouhan, O.P. Sharma, S. Kuriakose, S.A. Tawfik, M.J.S. Spencer, S. Walia, H. Sugimura, O.P. Khatri, Structural defects-mediated grafting of alkylamine on few-layer MoS_2 and its potential for enhancement of tribological properties, ACS. Appl. Mater. Inter., 12 (2020) 30720-30730, doi: 10.1021/acsami.0c08307.

[30] M.Z. Saidi, A. Pasc, C. El Moujahid, N. Canilho, M. Badawi, C. Delgado-Sanchez, A. Celzard, V. Fierro, R. Peignier, R. Kouitat-Njiwa, Improved tribological properties, thermal and colloidal stability of poly-α-olefins based lubricants with hydrophobic MoS_2 submicron additives, J. Colloid Interf. Sci., 562 (2020) 91-101, doi : 10.1016/j.jcis.2019.12.007.

[31] M. Li, D. Wang, J. Li, Z. Pan, H. Ma, Y. Jiang, Z. Tian, Facile hydrothermal synthesis of MoS_2 nano-sheets with controllable structures and enhanced catalytic performance for anthracene hydrogenation, RSC Adv., 6 (2016) 71534-71542, doi:10.1039/c6ra16084k.

[32] X. Zhang, Z. Du, X. Luo, A. Sun, Z. Wu, D. Wang, Template-free fabrication of hierarchical MoS_2/MoO_2 nanostructures as efficient catalysts for hydrogen production, Appl. Surf. Sci., 433 (2018) 723-729, doi:10.1016/j.apsusc.2017.10.105.

[33] D.N. Dunn, L.E. Seitzman, I.L. Singer, The origin of an anomalous, low 2θ peak in x-ray diffraction spectra of MoS_2 films grown by ion beam assisted deposition. J. Mater. Res., 12 (1997) 1191-1194, doi:10.1557/jmr.1997.0167.

[34] Z. Wu, D. Wang, A. Sun, Surfactant-assisted fabrication of MoS_2 nanospheres, J. Mater. Sci., 45 (2009) 182-187, doi:10.1007/s10853-009-3914-9.

[35] L. Ma, L. M. Xu, X. P. Zhou, X. Y. Xu, Biopolymer-assisted hydrothermal synthesis of flower-like MoS_2 microspheres and their supercapacitive properties, Mater. Lett., 132 (2014) 291-294, doi: 10.1016/j.matlet.2014.06.108.

[36] H. Yue, Y. Zhao, X. Ma, J. Gong, Ethylene glycol: properties, synthesis, and applications, Chem. Soc. Rev., 41 (2012) 4218-4244, doi:10.1039/c2cs15359a.

[37] H. Wang, X. Li, K. Yan, G. Liu, W. Song, T. Shen, D. Zou, Low-Temperature synthesis of near-monodisperse globular MoS_2 nanoparticles with sulphur powders, Nano, 12 (2017) doi:10.1142/s1793292017500916.

[38] X. Geng, W. Sun, W. Wu, B. Chen, A. Al-Hilo, M. Benamara, H. Zhu, F. Watanabe, J. Cui, T.-P. Chen, Pure and stable metallic phase molybdenum disulfide nanosheets for hydrogen evolution reaction, Nat. Comm., 7 (2016) 10672, doi:10.1038/ncomms10672.

[39] J. Polte, Fundamental growth principles of colloidal metal nanoparticles – a new perspective, Cryst. Eng. Comm., 17 (2015) 6809-6830, doi:10.1039/c5ce01014d.

[40] N. Akiya, P.E. Savage, Roles of water for chemical reactions in high-temperature water, Chem. Rev.,102 (2002) 2725-2750, doi:10.1021/cr000668w.

[41] P. Ramasamy, S.I. Mamum, J. Jang, J. Kim, Dopant induced diameter tuning of Mn-doped CdTe nanorods in aqueous solution, Cryst. Eng. Comm., 15 (2013) 2061-2066, doi:10.1039/c2ce26616d.

[42] S. Kumari, H.P. Mungse, R. Gusain, N. Kumar, H. Sugimura, O.P. Khatri, Octadecanethiol-grafted molybdenum disulfide nanosheets as oil-dispersible additive for reduction of friction and wear, FlatChem, 3 (2017) 16-25, doi:10.1016/j.flatc.2017.06.004.

[43] P. Afanasiev, I. Bezverkhy, Genesis of vesicle-like and tubular morphologies in inorganic precipitates: amorphous Mo oxysulfides, J. Phys. Chem. B., 107 (2003) 2678–2683, doi:10.1021/jp021655k.

[44] R.K. Yuldashev, K.M. Makhkamov, K.T. Sharipov, K.U. Aliev, Synthesis and study by IR and UV methods of spectral analysis of a complex of Mo(VI) with quercetin, Chem. Nat. Compd., 35 (1999) 420-421, doi: 10.1007/BF02282507.

[45] P.A. Gerakines, W.A. Schutte, J.M. Greenberg, E.F. Van Diishoeck, The infrared band strengths of H_2O, CO and CO_2 in laboratory simulations of astrophysical ice mixtures, Astron. Astrophys., 296 (1995) 810-818.

[46] X. Xu, J. Hu, Z. Yin, C. Xu, Photoanode Current of large-area MoS_2 ultrathin nanosheets with vertically mesh–shaped structure on indium tin oxide. ACS Appl. Mater. Inter., 6 (2014) 5983-5987, doi:10.1021/am501159s.

[47] P. Mao, Y. Wang, W. Guo, W. Zhang, T. He, S. Dong, P. Xiao, S. Rao, Morphology-controlled synthesis and lithium storage properties of SnO_2@C@MoS_2 hollow nanospheres with petaloid and granular MoS_2 nanosheets as the external layer in different solvents, J. Alloy. Compd., 850 (2021) 1567452, doi: 10.1016/j.jallcom.2020.156745.

[48] M. Hou, Y. Qiu, G. Yan, J. Wang, D. Zhan, X. Liu, J. Gao, L. Lai, Aging mechanism of MoS_2 nanosheets confined in N-doped mesoporous carbon spheres for sodium-ion batteries, Nano energy, 62 (2019) 299-309, doi:10.1016/j.nanoen.2019.05.048.

[49] X. Liu, X. Zhang, S. Ma, S. Tong, X. Han, H. Wang, Flexible amorphous MoS_2 nanoflakes / N-doped carbon microtubes /reduced graphite oxide composite paper as binder free anode for full cell lithium ion batteries, Electrochim. Acta., 333 (2020) 135568, doi: 10.1016/j.electacta.2019.135568.

[50] M. Yi, C. Zhang, The synthesis of two-dimensional MoS_2 nanosheets with enhanced tribological properties as oil additives, RSC Adv., 17 (2018) 9564-9573, doi: 10.1039/c7ra12897e.